Am J Transl Res 2019;11(5):2969-2982
www.ajtr.org /ISSN:1943-8141/AJTR0087947

Original Article

HIF-1-VEGF-Notch mediates angiogenesis in temporomandibular joint osteoarthritis

Yun Chen[1,2*], Bingjie Zhao[3*], Yong Zhu[1], Huaqiang Zhao[1], Chuan Ma[1]

[1]*Shandong Provincial Key Laboratory of Oral Tissue Regeneration, Department of Oral and Maxillofacial Surgery, School of Stomatology, Shandong University, Jinan, Shandong Province, China;* [2]*Jiangsu Key Laboratory of Oral Diseases, Nanjing Medical University, Department of Pediatric dentistry, Affiliated Hospital of Stomatology, Nanjing Medical University, Nanjing, Jiangsu Province, China;* [3]*Xuanwu Leader Dental Clinic, Nanjing, China.* [*]*Equal contributors.*

Received November 5, 2018; Accepted March 21, 2019; Epub May 15, 2019; Published May 30, 2019

Abstract: Angiogenesis has been reported participated in temporomandibular joint osteoarthritis (TMJ-OA). While the pathogenesis is unclear, recent studies indicate that hypoxia is important in TMJ-OA. In order to induce osteoarthritis-like lesions in mandibular condyles, rats were sleep deprived experimentally. An increased number of blood vessels were observed in the rats' condyles of SD and SR group compared with controls. Protein and mRNA levels of related factors including VEGF, HIF-1 and Notch were investigated by means of immunohistochemical staining, western blot and real-time PCR, which were highly expressed in the TMJ-OA rats. Furthermore, Cell test was designed to study effects of hypoxia on condylar chondrocytes. We found the expression of VEGF, HIF-1 and Notch were significantly increased in hypoxia group, indicating that HIF-1-Notch-VEGF signaling pathway were activated by hypoxia. The inhibitors of HIF-1 and Notch could suppress the expression of HIF-1, VEGF, Notch, suggesting the HIF-1-VEGF-Notch signaling pathway were bidirectional. Together, hypoxia played an important role in TMJ-OA and accelerates angiogenesis of condylar cartilage through HIF-1-VEGF-Notch signaling pathway. HIF-1α and Notch might be novel therapeutic targets in TMJ-OA.

Keywords: TMJ-OA, hypoxia, angiogenesis, HIF-1, Notch

Introduction

Osteoarthritis (OA) is a commonly and frequently encountered disease, characterized by progressive degradation of articular cartilage, osteophyte formation and synovial inflammation. Temporomandibular joint (TMJ) is one of the most common sites of OA; however, the pathogenic mechanisms of TMJ-OA are still unclear. Several studies found hypoxia involved in TMJ-OA, and stimulating the expression of vascular endothelial growth factor (VEGF) [1-3], which was closely related to angiogenesis. Meanwhile, angiogenesis of condylar cartilage and disc played an important role in the development of TMJ-OA [4].

Angiogenesis induced by hypoxia is mediated by a ubiquitous and highly conserved transcription factor, hypoxia inducible factor-1 (HIF-1) [5]. HIF-1 is a heterodimer consisting of a constitutively expressed β subunit and an oxygen-regulated α subunit, which primarily determines HIF-1 activation [6]. HIF-1α is degraded promptly under normoxic conditions but stabilized under hypoxic conditions, rapidly translocating to the nucleus, where it initiates the expression of VEGF [7]. Notch signaling pathway is a highly conserved intercellular pathway, which is another important pathway in angiogenesis [8]. VEGF could accelerate the expression of Notch receptor and activate Notch signaling pathway, and Notch could in turn affect the expression of VEGF. These interactions between VEGF and Notch signaling pathway play a vital role in angiogenesis.

Several studies have demonstrated that Notch signaling may interact with HIF-1 under hypoxia condition [9, 10], hypoxia could activate Notch-responsive promoters and up-regulate the expression of Notch downstream genes, such

as hairy and enhancer of split 1 (Hes1). Wei [11] further indicated that Notch-1/HIF-1α interactions mediated hypoxia-induced angiogenesis and invasion in inflammatory arthritis. Hypoxia-induced angiogenesis and endothelial cell function in vitro were Notch-1 dependent; Notch-1inhibitor could obviously weaken hypoxia-induced angiogenesis and endothelial cell function in vitro.

The present study was done to explore how hypoxia affects angiogenesis, and evaluate what role angiogenesis and HIF-1α, VEGF, Notch-1 play in TMJ-OA. TMJ-OA rat animal model was established, structure changes and angiogenesis of condylar cartilage were observed. The expression levels of related factors (HIF-1α, VEGF, Notch-1, Hes1) were detected. We also studied the effect of hypoxia on HIF-1/Notch-1 signaling pathway in chondrocytes, including the effects of HIF-1 or/and Notch-1 inhibition in vitro.

Materials and methods

Animal model

The modified multiple platform method (MMPM) was used to induce experimentally TMJ-OA rat model as previously described [12]. Briefly, the rats were put into a glass water tank contained 15 small platforms (diameter, 6.5 cm) or a grid (Figure S1). The grid was made of steel (about 2 cm apart), and it was used as environmental control. The tank was filled with water until approximately 1 cm from upper surface of the platforms or grid. Eight rats were placed in each tank, rats placed on the small platforms could jump from one to another, but when they reached the paradoxical phase of sleep, their faces would touch the water as the muscle atonia. Thus, the rats in the small platforms suffered from sleep deprivation continuously, meanwhile rats placed on the grid could lie down and sleep despite their tails might touch the water.

The rats could get chow pellets freely from a steel plate located upon the platforms or grid, since the major part of the plate was mesh structure other than the surrounding edge. The temperature of water and experimental room was controlled at 23°C and a 12:12 h light-dark cycle was created (lights on at 7:00 and off at 19:00). The water was changed daily and the rats were put into the tank for 18 h/d (starting at 16:00).

Animal experiment

One hundred and eighty male Wistar rats (8-week-old, weighting 200-220 g) were purchased from the Laboratory Animal Center of Shandong University (Jinan, China). The rats were randomly divided into 3 groups: the control groups (CN groups, n = 60), sleep deprivation groups (SD groups, n = 60), and the spontaneous recovery groups (SR groups, n = 60). The SD and SR rats were placed on small platforms to achieve sleep deprivation, while the CN rats were placed on the grid. The rats were acquainted with the library conditions for one week and adapted to the model for 30 min/d for another week prior to the start of experiment.

The SD and CN rats were sacrificed at the end of 4th, 6th and 8th week after the beginning of the experiment (20 rats per subgroup), and they were defined as SD4, SD6, SD8, CN4, CN6, CN8 subgroup. While the SR rats suffering from sleep deprivation until the end of 4th, 6th and 8th week; subsequently were sacrificed after one week of recovery by housed in the cages (20 rats per subgroup), and they were defined as SR4, SR6, SR8. All the animals were sacrificed by injection of overdose pentobarbital sodium and their bilateral condyles were removed. All the experimental procedures performed in this study were approved by the Committee on the Ethics of Animal Experiments of Jinan Military General Hospital (No. IACUC-2013-001). All surgery was performed under sodium pentobarbital anesthesia, and we have tried our best to minimize rat suffering.

Tissue preparation

Eight rats of each subgroup were randomly selected and their bilateral condyles with surrounding tissues were resected, fixed in 10% buffered paraformaldehyde and decalcified with 10% EDTA for 4 weeks at 4°C. Then they were embedded in paraffin, and sagittal sections (5 μm) were cut in the midpoint of the joint. The sections were used for hematoxylin and eosin (HE) and immunohistochemical staining.

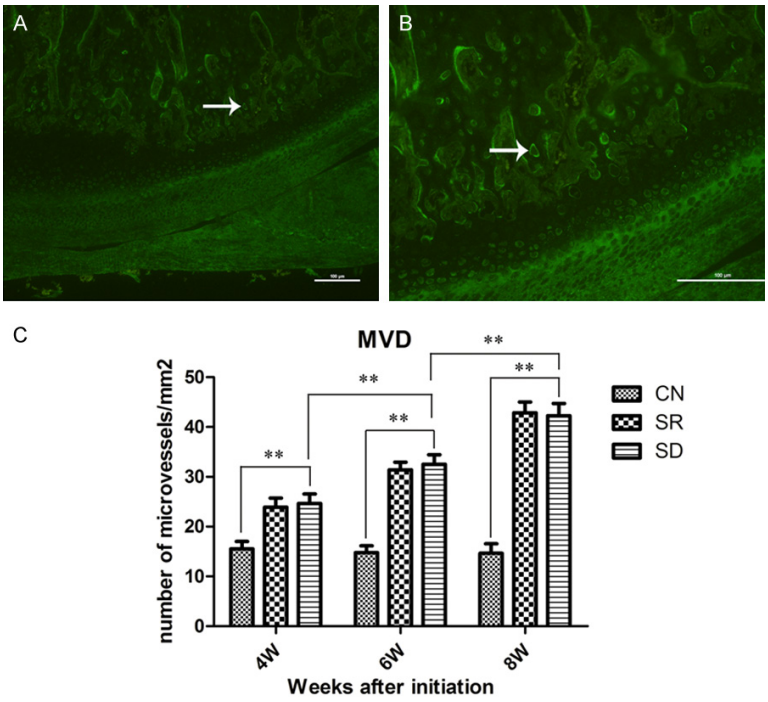

Figure 1. Angiogenesis at the osteochondral junction. (A, B) Representative images of immunofluoresense staining showed the vessels at the osteochondral junction in different views. White arrows indicated a same vessel. Original magnification ×100 (A) and ×200 (B), scale bars = 100 μm. (C) The micro vessel density (MVD) in all groups. MVDs of the SD groups were higher than CN groups, and increase in a time-dependent manner. Bars represent the mean ± SD of each group. Significant differences between the groups are marked with asterisks. (* = $P < 0.05$, ** = $P < 0.01$).

The condyles of the other twelve rats in each subgroup were immediately frozen in liquid nitrogen and stored at -80°C. Among these rats, six were randomly selected for Western Blot analysis, another six were used for real-time quantitative reverse transcription polymerase chain reaction (RT-PCR) analysis. Bilateral condyles of each rat were collected as one sample, ensuring that protein or RNA was sufficient for analysis.

Immunohistochemistry

To examine the expression of HIF-1α, Notch-1 and VEGF and their localized distribution, immunohistochemical staining was performed on routinely process. Briefly, the sections were dewaxed in xylene, rehydrated, and pretreated with 3% hydrogen peroxide in methanol. Microwave treated antigen retrieval was performed and non-specific binding was blocked using goat serum for 30 min, and the slides were then incubated overnight at 4°C with primary antibodies including those that HIF-1α (Novus Biological, NB100-449, USA), Cleaved Notch-1 [Notch-1 intracellular domain, NICD (Cell Signaling Technology, #2421, USA)] and VEGF (Abcam, ab46154, USA). Antibody binding was localized using a secondary biotin-labeled anti-rabbit antibody and the streptavidin-conjugated horseradish peroxidase (Bohai biotechnology, China), and revealed using 3, 3'-diaminobenzidine as the chromogenic substrate for peroxidase. The slides were then rinsed with phosphate buffer solution (PBS), and counterstained with hematoxylin, dehydrated, cleared, and mounted.

Micro vessel density (MVD)

MVD of osteochondral junction was evaluated with CD-105 which was regarding as endoglin, and immunofluoresense was performed. Briefly, the sections were dewaxed in xylene, rehydrated, and pretreated with 3% hydrogen peroxide in methanol. Microwave treated antigen retrieval was performed and non-specific binding was blocked using goat serum for 30 min, and the slides were then incubated overnight at 4°C with rabbit anti-CD105 polyclonal antibodies (Boster, BA2227, China). Fluorescently-labeled anti-rabbit antibody was then used, rinsed with PBS, dried and mounted.

MVD was assessed according to Weidner's [13] method. Briefly, the sections were scanned at 100× magnification to select the three most highly vascularized areas ("hot spots"), in which the micro-vessels were counted at 200× magnification and their density indicated the mean number of micro-vessels/mm^2. Any luminous single endothelial cell or cell cluster, with or without a discernible lumen, which was clearly separated from the adjacent micro-vessels, cells or other connective tissue elements was

Table 1. Simplified scoring scale for HIF-1α, VEGF and NICD

Score	Criteria		
	HIF-1α	VEGF	NICD
0	No positive expression	Fewer more than 50% of deep chondrocytes positive	No positive expression
1	Some, but fewer more than 50% of deep chondrocytes positive	50% or more of the deep chondrocytes positive	Fewer more than 50% of deep chondrocytes positive
2	50% or more of the deep chondrocytes positive	Positive chondrocytes in the deep and intermediate zones	50% or more of the deep chondrocytes positive
3	Positive chondrocytes in the deep and intermediate zones, even into the superficial zone	Positive chondrocytes in the deep, intermediate and superficial zones	Positive chondrocytes in the deep and intermediate zones

regarded as a countable vessel (**Figure 1A**, **1B**).

Histological scores

HE, immunohistochemical and immunofluoresense staining sections were observed using a light microscope (DM 2500, Leica, Germany), MVD and histological scores were counted by two independent viewers. Chondropathy scores were evaluated according to Janusz's method [14]. The cartilage damage was scored as follow: 0. Normal, Cartilage with normal appearance; 1. Minimal, superficial zone only; 2. Mild, extends into the upper middle zone; 3. Moderate, well into the middle zone; 4. Marked, into the deep zone but not to tidemark; 5. Severe, full thickness degeneration to tidemark. The amount of cartilage damage was assessed as 1/3, 2/3 or major (>2/3) of the surface of the condylar cartilage, and the above score multiplied by 1, 2 or 3 respectively to get a total chondropathy score.

Scores of immunoreactivities for HIF-1α, VEGF and NICD were also counted and the scoring systems were devised based on initial qualitative analysis (**Table 1**) depending on percentage and/or location of immunoreactive chondrocytes.

Western blot

Ground up and mixed with RIPA lysis buffer (Beyotime, China) and 1 mmol/L phenylmethanesulfonyl fluoride (PMSF), condyles were then homogenized in a gentle MACSTM Dissociator (Miltenyl Biotec, Germany). The samples were centrifuged at 15,000 r/min, 4°C for 10 min to get supernatant for future determination. The protein concentrations were measured using a BCA kit (Beyotime, China), and then 50 μg protein samples were subjected to sodium dodecyl sulfate-polyacrylamide (10%) gel electrophoresis (SDS-PAGE) using a tris-glycine running buffer. Subsequently, they were transferred onto a polyvinylidenefluoride (PVDF) membrane (Solarbio, China). The membrane was blocked in blocking buffer [5% nonfat milk in trisbuffered saline containing 0.05% Tween-20 (TBST)] at room temperature for 2 h, and then incubated overnight at 4°C with primary antibodies including those that HIF-1α (Novus Biological), NICD (Cell Signaling Technology), VEGF (Abcam) and β-actin (Beyotime, AA128, China). After washing three times (5 min per wash) with TBST, the membrane was incubated with a horse radish peroxidase-conjugated secondary antibody (Bioworld, BS-13278, USA or Beyotime, A0126, China). The membrane was washed three times (5 min per wash) with TBST again, and enhanced chemiluminescence using an ECL chemiluminescence kit (Beyotime, China). The blots were exposed to autoradiographic film for 1-2 min for detection.

RT-PCR

Total RNA was prepared using Trizol reagent (Sangon Biotech, SK1311, China), following the manufacturer's instruction. GADPH was used as an endogenous control, and target gene primers were designed as follows: HIF-1α, CGATGACACGGAAACTGAAG (forward) and CAGAGGCAGGTAATGGAGACA (reverse); VEGF, CCGGTTTAAATCCTGGAGCG (forward) and TTTAACTCAAGCTGCCTCGC (reverse); Notch-1, GTGAGTGGGATGGACTGGAC (forward) and GGAAGGAGTTGTTGCGTAGC (reverse); Hes1, GTGGGTCCTAACGCAGTGTC (forward) and TCAG-

AAGAGAGAGGTGGGCTA (reverse); GADPH, ATGATTCTACCCACGGCAAG (forward) and CTGGAAGATGGTGATGGGTT (reverse). Reverse transcription and real-time PCR were performed in a reaction volume of 20 μL by using PrimeScript™ RT Reagent Kit (Perfect Real Time) (TaKaRa, RR037A, Japan) and SYBR® Premix Ex Taq™ II (Tli RNase H Plus) (TaKaRa, RR820A, Japan) according to the manufacturer's instruction. Assays were performed in triplicates using default program and the expression levels of the target genes relative to GADPH were calculated by the formula $2^{-\Delta\Delta Ct}$, the CN4 subgroup was used as the calibrator.

Cell culture

The dissections harvested from ten 3-week-old Wistar rats TMJ condyles were minced and digested in 0.25% trypsin (Invitrogen, USA) at 37°C for 10 min. Centrifuged deposit was incubated in 0.2% collagen II (Invitrogen, USA) for 2 h. Subsequently, the condylar chondrocytes were washed and resuspended in Dulbecco's Modified Eagle Medium [DMEM (sigma, USA)] containing 10% fetal bovine serum [FBS (sigma, USA)], penicillin/streptomycin (100 unites/ml) and were used for experiments between passages 3 and 5.

Chondrocytes were placed at 1×10^6 cells/well in 6-well plates, and cultured at 37°C in a humidified incubator or hypoxia chamber, and divided into four groups: N group (cultured under normoxic condition, 21% O_2, 5% CO_2 and 74% N_2); H group (cultured under hypoxia condition, 1% O_2, 5% CO_2 and 94% N_2); H+Y group [cultured under hypoxia condition in media with 50 μM (3-(50-hydroxymethyl-20-furyl)-1-benzyl indazole (YC-1), specific HIF-1α inhibitor; sigma, USA)]; H+D group [cultured under hypoxia condition in media with 50 μM DAPT (γ-secretase inhibitor which was usually used to block Notch signaling pathway; sigma, USA)]. After cultured for 24 h under experimental conditions, the expression levels of HIF-1α, NICD/Notch-1, VEGF and Hes1 were assessed by Western Blot and RT-PCR as previously described (The N group was used as the calibrator).

Statistical analysis

Statistical analysis was performed using Statistical Package for Social Scientists (SPSS) version 13.0 software (SPSS inc., Chicago, USA). Histological scores (scores of immunoreactivities and chondropathy scores) were recorded as median and inter-quartile range (IQR), and analyzed by Mann-Whitney U tests. Experimental data of RT-PCR, Western Blot and MVD were recorded as means with 95% confidence interval (CI) and analyzed by student's t-test or one-way ANOVA followed by Dennett's or Turkey's post-test. Associations between variables are expressed as Spearman's correlation coefficients. *P*-value of less than 0.05 was considered statistically significant.

Results

TMJ-OA rat model was successfully established

In control (CN) groups, normal appearance of the condylar cartilages was observed by haematoxylin and eosin (HE) staining, the surface was smooth and chondrocytes were evenly distributed inside cartilage as four layers, no obvious histopathological changes were found. While the sleep deprivation (SD) groups showed features of OA-like histopathological changes, e.g. loss of cartilage surface integrity, reduction and disarrangement of chondrocytes, cluster formation and cell-free area (**Figure 2**). In addition, osteophyte-like formation was also found in 2 rats (out of 8) of SD 8-week subgroup. OA-like pathological changes of SD groups showed progressive enhancement with time. In the spontaneous recovery (SR) groups, histopathological changes such as irregular surface, disarrangement, and cell clusters were also observed, but they were milder and uncommon compared with SD groups.

The chondropathy scores of SD groups were significant higher than CN groups at three times, and increased in a time-dependent manner (SD6/SD4: $P = 0.013$, SD8/SD6: $P = 0.019$). The scores of the CN group was 0, 0-0 (median and inter-quartile range), the scores of SR group (3.5, 2.25-4) increased significantly ($P < 0.01$), while lower than SD group (6, 4-6) at 8 week.

These findings confirmed that sleep deprivation could cause OA-like pathological changes of rat TMJ, which might be reversible at the early stage.

Angiogenesis at osteochondral junction

In CN groups, blood vessels were clearly confined within the calcified cartilage layer using

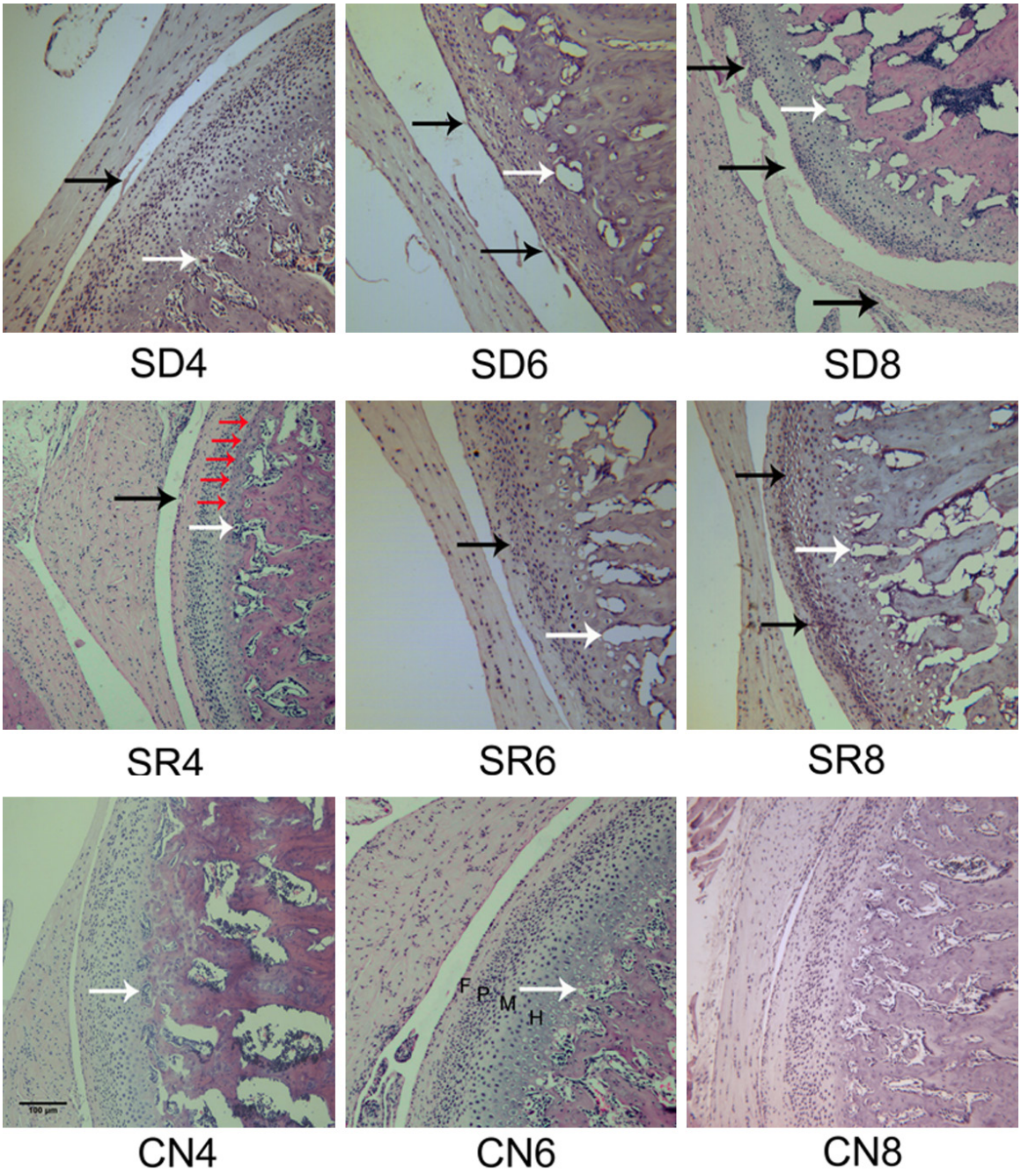

Figure 2. Rats TMJ sections of HE staining. (A) In CN groups, the condylar cartilage displayed normal appearance, the articular surface was smooth and chondrocytes were homogenously distributed throughout the cartilage. Condylar cartilage could be clearly distinguished as four layers, fibrous layer (F), proliferating cell layer (P), mature cell layer (M), hypertrophic cell layer (H). While histopathological changes, such as loss of cartilage surface integrity reduction and disarrangement of chondrocytes, cluster formation and cell-free area (black arrows) were observed in SR and SD groups. Blood vessels at the osteochondral junction are indicated by white arrows. The tidemark was indicated by red arrows. Scale bars = 100 μm, original magnification ×100.

immunofluorescence and HE staining, below the tidemark (junction of calcified cartilage and noncalcified cartilage) (**Figure 2**). Contrasted with CN group, an increased number of blood vessels were found at osteochondral junction of the rats' condyle in SD and SR group (**Figures 1A**, **1B**, **2**). A few number of blood vessels reached into the non-calcified cartilage in SD

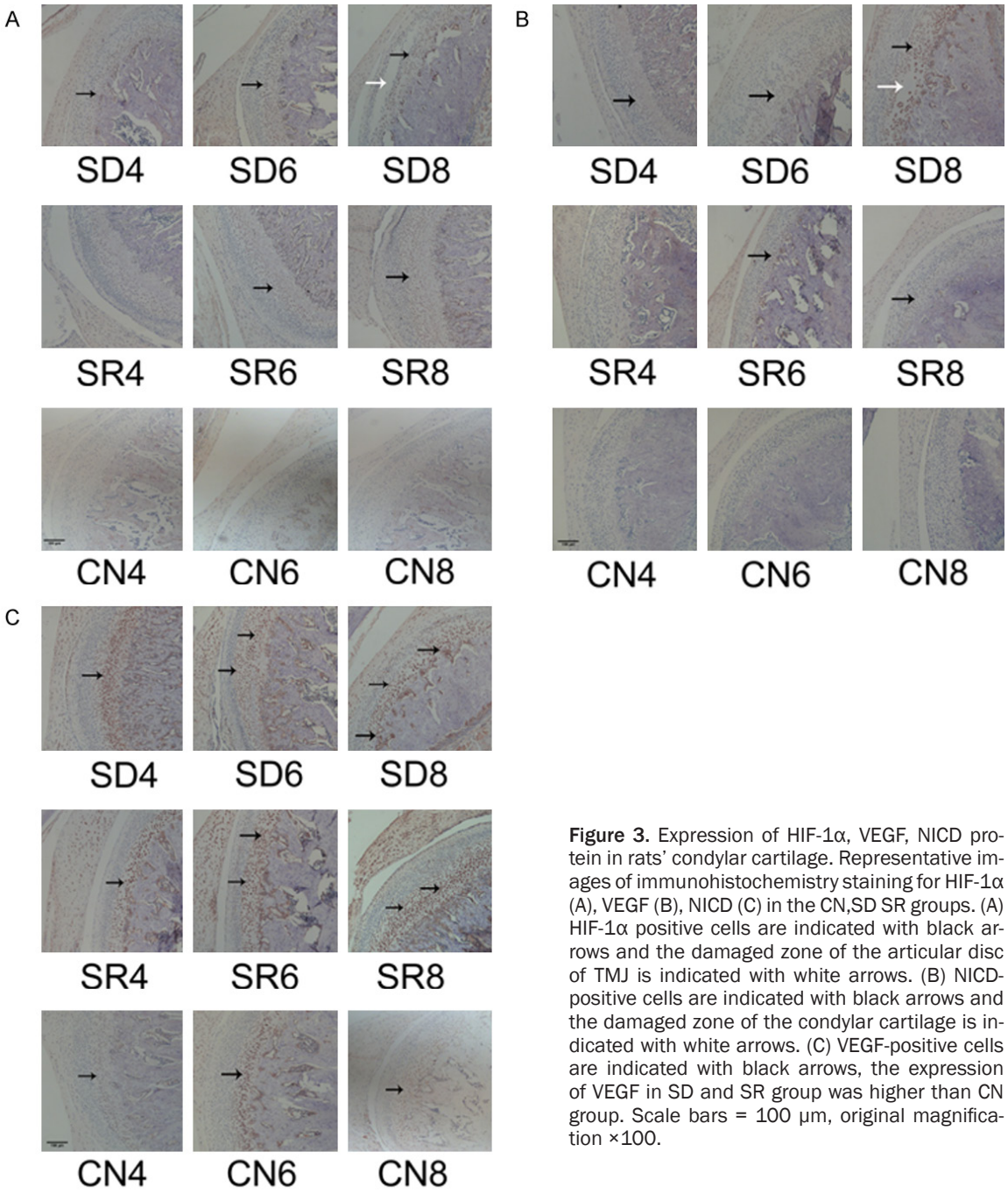

Figure 3. Expression of HIF-1α, VEGF, NICD protein in rats' condylar cartilage. Representative images of immunohistochemistry staining for HIF-1α (A), VEGF (B), NICD (C) in the CN,SD SR groups. (A) HIF-1α positive cells are indicated with black arrows and the damaged zone of the articular disc of TMJ is indicated with white arrows. (B) NICD-positive cells are indicated with black arrows and the damaged zone of the condylar cartilage is indicated with white arrows. (C) VEGF-positive cells are indicated with black arrows, the expression of VEGF in SD and SR group was higher than CN group. Scale bars = 100 μm, original magnification ×100.

and SR group at 8 week, but the blood vessels of CN group just located limited in the calcified cartilage.

The micro vessel density (MVD) in the osteochondral junction was calculated in all groups. The mean MVDs of SD groups were significantly higher than CN groups, similar to SR groups (**Figure 1C**). The MVD in SD group (24.65, 22.75-26.55) was greater than CN group (15.54, 14.04-17.03) at 4 weeks ($P < 0.01$). Moreover, the MVD in SD group at 8 week (42.26, 39.80-44.73) was higher than that at 4 weeks (24.65, 22.75-26.55) ($P < 0.01$). MVD were also increased in a time-dependent manner in both SD and SR groups.

These results show that the blood vessels was increased and breached into non-calcified cartilage in the rats' TMJ after sleep deprivation. Therefore, sleep deprivation can promote angiogenesis in the TMJ.

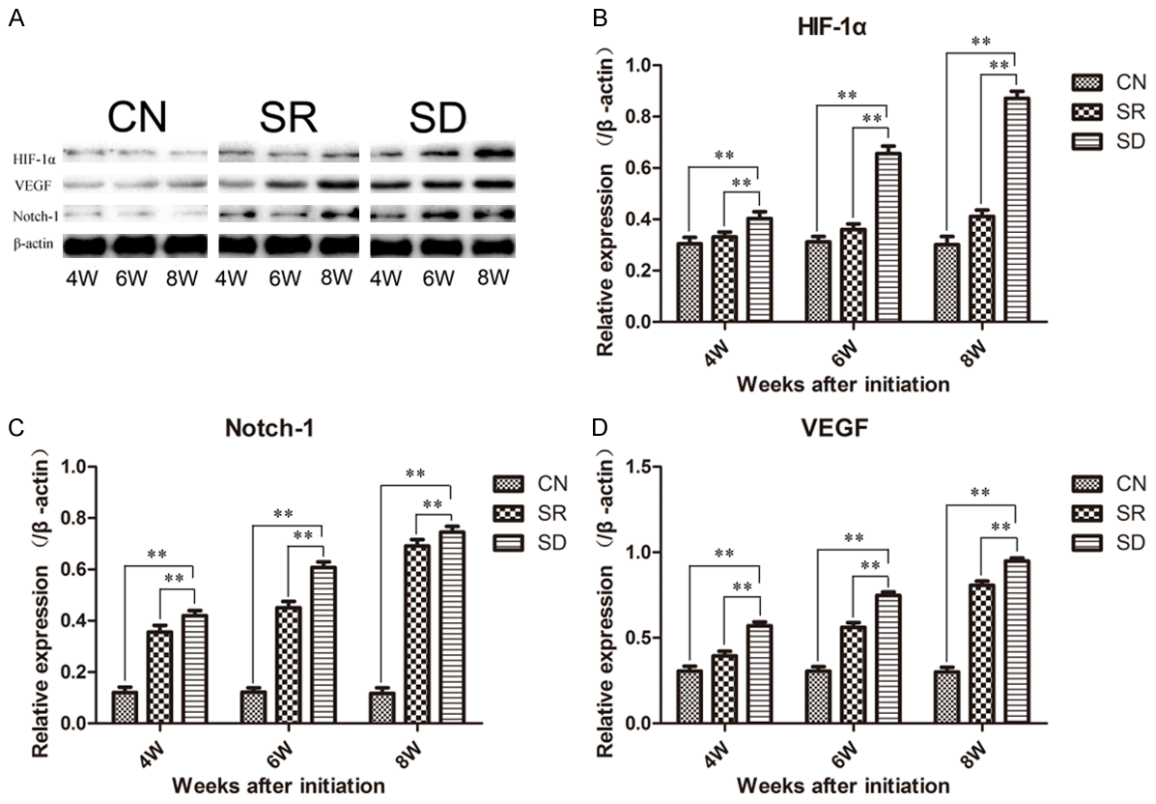

Figure 4. Western Blot showed the expression levels of HIF-1α, Notch-1, and VEGF in rats' condylar cartilages. (A) Representative images of Western Blot and the expression levels of HIF-1α (B), VEGF (C) and Notch-1 (D) proteins data were normalized to β-actin protein levels. The expression of HIF-1α, VEGF, and Notch-1 in rats' condylar cartilages after sleep deprivation was up-regulated, but down-regulated after one week recovery. Bars show the mean ± 95% CI, * = < 0.05, ** = P < 0.01.

HIF-1, Notch, VEGF expression were increased in the TMJ-OA

Immunohistochemical staining showed that the expression levels of HIF-1α, NICD and VEGF were relativity stronger in SR8, SD6 and SD8 subgroups; while were weaker, or even negative in SR4, SR6, SD4 subgroups and CN groups (**Figures 3**, S5, S6 and S7). Positive expression of HIF-1α and NICD were observed in both cytoplasm and nucleus, especially concentrated on the chondrocytes of mature, hypertrophic layer and cubical cells around blood vessels of osteochondral junction.

Western Blot revealed that the three proteins (HIF-1α, NICD, and VEGF) expressed in similar way, the expression levels of SD groups were higher than CN groups, and SR groups were lower than SD groups. And they increased as time evolved in both SD and SR groups, but with little variation in CN groups (**Figures 4**, S2 and S3). The notion was further proven by the scores of immunoreactivities.

mRNA expression levels of HIF-1α, VEGF, Notch-1 and Hes1 in condylar cartilage were detected by RT-PCR. The expression levels of all the four mRNAs also showed the similar pattern as their relative proteins (**Figure 5**). Levels of SR and SD group were higher than CN group, and levels of SD group were higher than SR group. At the meantime, these distinctions became even more marked as time prolonged.

Angiogenesis and HIF-1, Notch, VEGF were close correlated

Associations between these variables (MVD and HIF-1, Notch, VEGF) are expressed as Spearman's correlation coefficients. Spearman's correlation coefficients revealed that MVD increased with the increase of chondropathy scores and HIF-1α, NICD, VEGF scores in SD groups (**Table 2**), but not in SR groups.

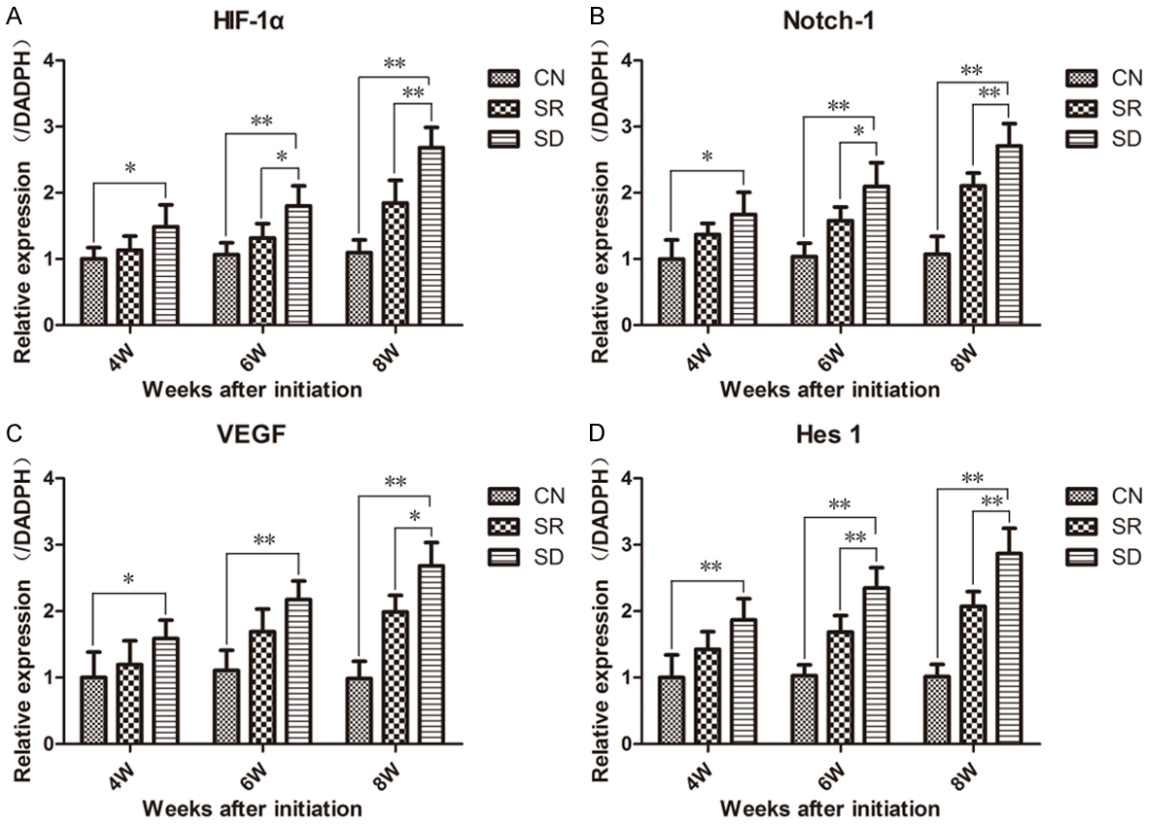

Figure 5. RT-PCR showed the expression levels of HIF-1α (A), VEGF (B), Notch-1 (C) and Hes1 (D) mRNA in rats' condylar cartilage. Sleep deprivation induced high expression of HIF-1α, VEGF, Notch-1 and Hes1 in rats' condylar cartilages. The formula $2^{-\Delta\Delta Ct}$ was used with GADPH as internal reference. Bars show the mean ± 95% CI, * = < 0.05, ** = P < 0.01.

Table 2. Relationship between each investigated index of SR and SD groups

SR group	Chondropathy scores	MVD	HIF-1#	Notch-1#
MVD	0.402			
HIF-1#	0.529**	0.158		
Notch-1#	0.425*	0.134	0.342	
VEGF#	0.425*	0.134	0.342	1.0**
SD group	Chondropathy scores	MVD	HIF-1#	Notch-1#
MVD	0.788**			
HIF-1#	0.850**	0.626**		
Notch-1#	0.785**	0.576**	0.758**	
VEGF#	0.661**	0.627**	0.508*	0.636**

Numerical values are Spearman's correlation coefficients. #Means scores of immunoreactivities of HIF-1, Notch-1 and VEGF, respectively. *P < 0.05; **P < 0.01.

Meanwhile, spearman's correlation coefficients indicated that the expression of the four mRNAs were highly correlative with each other (**Table 3**).

In conclusion, positive expression of HIF-1α and NICD were observed in nucleus demonstrated that HIF-1 and Notch signaling pathway were exactly activated, results of our Western Blot and PCR proved it again. HIF-1α, NICD, VEGF scores highly correlated with MVD and their positive expression concentrated in vascular endothelial cell, which stated they were closely related to angiogenesis. High positive correlation of the four mRNAs also gave evidence for HIF-1-VEGF-Notch signaling pathway in TMJ-OA, just as we had hypothesized. Thus, we confirmed angiogenesis and HIF-1-Notch-VEGF signaling pathway played an important role in development of TMJ-OA.

Hypoxia induces high expression of HIF-1α, VEGF and Notch-1 in chondrocytes

Chondrocytes were well cultured in a humidified incubator or hypoxia chamber. After cultured under experimental conditions for 24 hours, the expression levels of HIF-1α, NICD/

Table 3. Relationship between mRNA expression levels of interrelated factors of all groups

	HIF-1α	Notch-1	VEGF
Notch-1	0.772**		
VEGF	0.810**	0.818**	
Hes1	0.870**	0.879**	0.866**

Numerical values are Spearman's correlation coefficients. **P < 0.01.

Notch-1, VEGF and Hes1 were assessed by Western Blot and RT-PCR.

Western Blot showed the three proteins (HIF-1α, NICD, and VEGF) expressed in similar way, highest expression in hypoxia group and significantly higher than those of N (normoxic condition) group. In H+Y (hypoxia+YC-1, inhibitor of HIF-1) group and H+D (hypoxia+DAPH, inhibitor of Notch-1) group, the expression levels of the three proteins were significantly less than hypoxia group, but significantly higher than N group (**Figures 6A**, **6B** and S3, S4).

RT-PCR revealed that the expression levels of HIF-1α, VEGF, Notch-1 and Hes1 were agree with their relative proteins, hypoxia group were significantly higher than H+Y group and H+D group, than N group (**Figure 6C**). The difference between H+Y group and H+D group has no statistically significance.

Proteins and mRNAs expression levels of hypoxia group were significantly higher than N group, stated that HIF-1-Notch-VEGF signaling pathway were activated by hypoxia. H+Y group were lower than hypoxia group demonstrated that blocking HIF-1 signaling pathway could suppress HIF-1-Notch-VEGF in hypoxia condition. While H+D group were also lower than hypoxia group indicated that controlling Notch signaling pathway could get the same effect, Notch could also in turn affect HIF-1-VEGF-Notch signaling pathway. These results suggested HIF-1 and Notch interacted with each other, and the HIF-1-VEGF-Notch signaling pathway were bidirectional.

Discussion

Angiogenesis of articular cartilage has been found to be one of the earliest changes and conduced to other features of OA in the knee joint [15]. In normal joints, the micro blood vessels are rarely detected in the non-calcified cartilage beyond the tidemark (junction of calcified cartilage and noncalcified cartilage) [16]. But in OA, several recent studies have indicated that the micro vessels from the subchondral bone can breach the tidemark and invade into the non-calcified cartilage [16-18]. In addition, osteophyte formation, one of the typical changes in OA joint, is believed to be angiogenesis-dependent. Several other studies also found that angiogenesis played an important role in the development of TMJ-OA [1, 4], but the exact regulatory mechanisms were still unclear.

Angiogenesis of TMJ cartilage could create hypoxic environment, HIF-1 would be activated and up-regulated expression of VEGF, which was closely related to angiogenesis [1, 3]. Considering that Notch signaling pathway was another important pathway in angiogenesis and VEGF was positive regulatory factor of Notch [19], we speculated that HIF-1-VEGF-Notch signaling pathway participated in angiogenesis of TMJ condylar cartilage for the first time.

Many studies have showed that psychological factors, such as sleep disorders, psychological stress, and depression, were related to TMJ dysfunction [20-22]. In our previous study, MMPM have been used to establish a sleep deprivation model of rats, and caused pathological alterations in rats' TMJ [12]. In the present study, we increased the time of sleep deprivation, OA-like lesions were found in the rats' condyles, and angiogenesis in osteochondral junction was also detected. And the number of blood vessels at the osteochondral junction is markedly increased in SD groups compared with CN groups. Our findings demonstrated that angiogenesis also promoted development of TMJ-OA caused by psychological factor.

We found histopathological changes such as irregular surface, disarrangement, and cell clusters in the SR groups were more unapparent and uncommon compared with SD groups. Thus we speculated TMJ-OA could be reversed and treated at the early stage. It differed from the traditional view that OA was not reversible, could be interpreted that TMJ was a special structure over other synovial joints in that it required constant remodeling throughout life [23], which need more studies to testify.

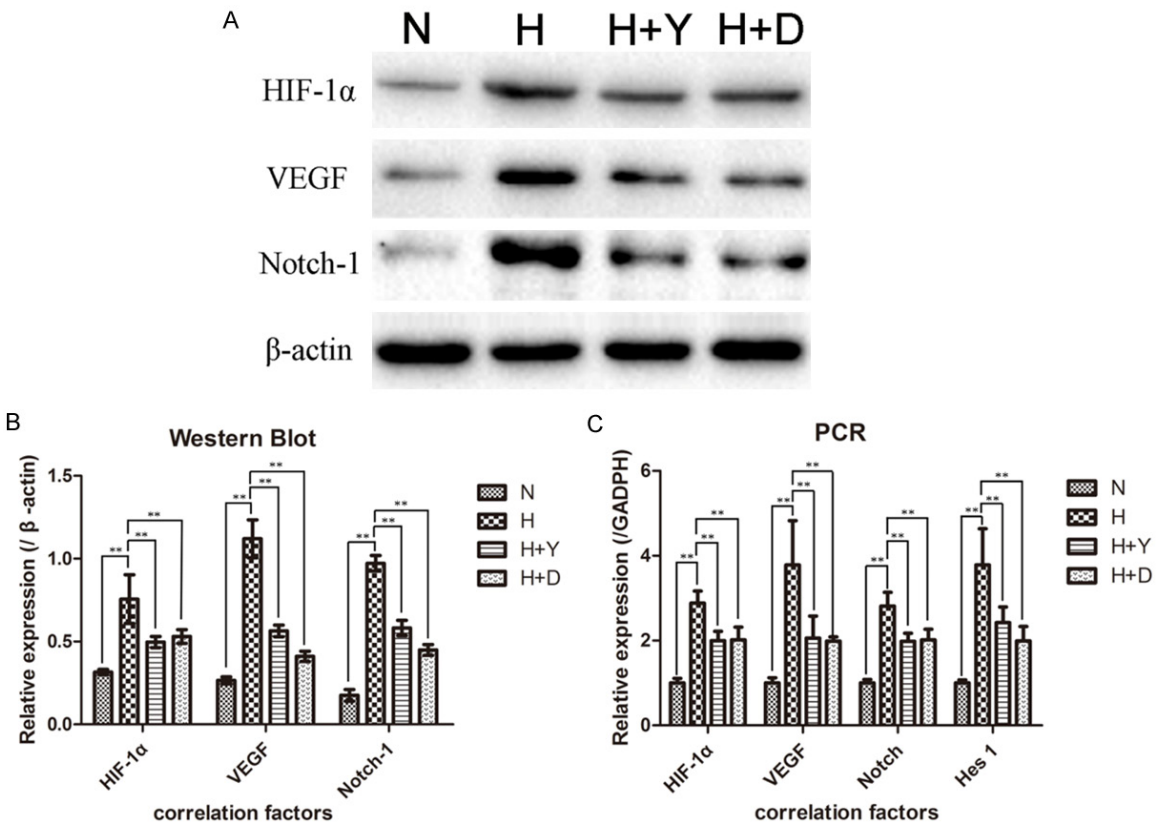

Figure 6. Hypoxia induces high expression of HIF-1α, VEGF and Notch-1 in chondrocytes. Western Blot and RT-PCR showed the expression of related factors in chondrocytes of N (normoxia), H (hypoxia), H+Y and H+D group. (A) Representative Western Blot of HIF-1α, VEGF and Notch-1 in chondrocytes and (B) Western Blot data were normalized to β-actin protein levels. The expression levels of HIF-1α, VEGF and Notch-1 proteins of H group significantly higher than N group indicated that HIF-1-Notch-VEGF axis was activated. When adding the inhibitor of HIF-1α or Notch-1, HIF-1-Notch-VEGF axis was suppressed. (C) The mRNA expression levels of HIF-1α, VEGF, Notch-1 and Hes-1 in different groups. The $2^{-\Delta\Delta Ct}$ method was adopted with GAPDH as the reference gene. They changed in accord with their relative proteins. Bars represent the mean ± SD of each group (n = 8). Bars show the mean ± 95% CI, ** = P < 0.01.

MVDs were not correlated with the chondropathy scores and HIF-1α, VEGF, Notch-1 scores in SR groups, and mean MVDs were slightly lower than that of SD groups which suggest that rats in SR groups rested for only one week without any sleep deprivation or treatments, the vessels have not been degraded though HIF-1α, VEGF, Notch-1 expression were decreased. While angiogenesis could promote OA, it was also a crucial step of TMJ remodeling which alleviate the histopathological changes of condylar cartilage, this could be another reason for MVDs were still higher, when the other indicators down-regulated [24].

Both receptors and ligands of Notch were transmembrane proteins, when Notch-1 was activated by binding of ligand to receptor, NICD (Notch-1 intracellular domain) would be split off and translocated to the nucleus where it initiated the expression of downstream genes, which process was similar to HIF-1α [7, 25]. Our Western Blot, RT-PCR data showed high HIF-1α and Notch expression in SD group, and immunohistochemistry showed that HIF-1α, NICD positive expression mainly concentrated in nucleus. These demonstrated HIF-1 and Notch-1 were actually activated. The previous studies have shown that VEGF was downstream gene of HIF-1, and could induce the activation of Notch-1 [7, 26, 27]. In the present study Spearman's correlation coefficients revealed the association between HIF-1α, VEGF, Notch-1, Hes1, MVD and chondropathy scores were highly correlated. We could indicate that HIF-1-VEGF-Notch signaling pathway played a vital role in angiogenesis of condylar cartilage and accelerated the development of TMJ-OA, as we hypothesized.

Most studies about HIF-1 and Notch signaling pathway focused on malignancies, several recent studies have explored their effects in the pathogenesis of OA, respectively [1, 3, 28-31]. The association between HIF-1 and Notch signaling pathway in RA have been well established [11], but for now there is no study on this aspect in OA. In the present study, HIF-1α and Notch-1 were found over-expressed in condylar cartilages of TMJ-OA rats, and interaction between HIF-1α and Notch-1 were further studied, our findings filled the research gap in OA.

HIF-1α would be degraded promptly under normoxic conditions, so we inferred hypoxia got involved in the development of TMJ-OA, agreeing with the studies of Nitzan [32] and Yamaguchi [29]. Cernanec and Chang have demonstrated that hypoxia was one of the major pathogenesis factors in both OA and RA in the knee joints [33, 34]. Our cell experiment indicated that HIF-1 signaling pathway was activated under hypoxia condition, and then induced VEGF and Notch signaling pathway. Proteins and mRNAs (HIF-1α, Notch, and VEGF) expression levels in hypoxia group were significantly increased, which stated that HIF-1-Notch-VEGF signaling pathway was activated. Moreover, use of YC-1 and DAPT could restrain expression of the related genes and proteins, which demonstrated that HIF-1 and Notch signaling pathway interacted with each other. Blocking of HIF-1 or Notch both could interrupt HIF-1-VEGF-Notch signaling pathway, at least in part.

The inhibition of HIF-1α has been proven effective in curing OA and RA in vivo and in vitro [28, 35]. VEGF, the downstream gene of HIF-1 and the most important factor in angiogenesis, its role in treating inflammatory diseases (including OA) and malignant tumor has received widespread accepted [1, 8, 36]. Arne [37] has proven that VEGF was a fascinating target in anti-angiogenic therapies for RA. Moreover, Notch signaling pathway, was also considered to be a target of anti-angiogenic therapies for RA [11], and got excellent outcomes.

Above all, we conjecture that HIF-1 and Notch might be used as target of anti-angiogenic therapies for TMJ-OA, and gave new novel ideals for clinical treatments and/or control for TMJ-OA, especially at the early stage. However, more animal and clinical experiments are needed, and we will continue to explore in the future.

Our study has a few limitations like other researches in animal models. Firstly, two other groups of rats were designed to receive intra-articular injection of YC-1 or DAPT originally, the mortality of the rats was so high that they were cancelled; the effects of the inhibitors on TMJ-OA in rats could not be studied. Secondly, the time-series detection and comparison were done at 2-week intervals, and the rats suffered from sleep deprivation for only 8 weeks. Longer-term sleep deprivation and shorter intervals would be considered in later researches.

Acknowledgements

Supported by the Natural Science Foundation of Shandong Province (Grant No. ZR2018PH-022) and Medical Science and Technology Development Plans of Shandong province (No. 2017WS481).

Disclosure of conflict of interest

None.

Address correspondence to: Chuan Ma and Huaqiang Zhao, Department of Oral and Maxillofacial Surgery, College of Stomatology, Shandong University, Number 44, Wen Hua Xi Road, Jinan 250012, Shandong Province, China. Tel: +86 18888308321; Fax: +86 531 88382923; E-mail: machuan0817@163.com (CM); Tel: +86 13506402199; Fax: +86 531 88382923; E-mail: zhaohq@sdu.edu.cn (HQZ)

References

[1] Shirakura M, Tanimoto K, Eguchi H, Miyauchi M, Nakamura H, Hiyama K, Tanimoto K, Tanaka E, Takata T and Tanne K. Activation of the hypoxia-inducible factor-1 in overloaded temporomandibular joint, and induction of osteoclastogenesis. Biochem Biophys Res Commun 2010; 393: 800-805.

[2] Milam SB and Schmitz JP. Molecular-biology of temporomandibular-joint disorders - proposed mechanisms of disease. J Oral Maxillofac Surg 1995; 53: 1448-1454.

[3] Ke J, Liu Y, Long X, Li J, Fang W, Meng QG and Zhang YF. Up-regulation of vascular endothelial growth factor in synovial fibroblasts from human temporomandibular joint by hypoxia. J Oral Pathol Med 2007; 36: 290-296.

[4] Wang QY, Dai J, Kuang B, Zhang J, Yu SB, Duan YZ and Wang MQ. Osteochondral angiogenesis

in rat mandibular condyles with osteoarthritis-like changes. Arch Oral Biol 2012; 57: 620-629.
[5] Huang LE, Arany Z, Livingston DM and Bunn HF. Activation of hypoxia-inducible transcription factor depends primarily upon redox-sensitive stabilization of its alpha subunit. J Biol Chem 1996; 271: 32253-32259.
[6] Cheng YL, Park JS, Manzanero S, Choi Y, Baik SH, Okun E, Gelderblom M, Fann DY, Magnus T, Launikonis BS, Mattson MP, Sobey CG, Jo DG and Arumugam TV. Evidence that collaboration between HIF-1 alpha and Notch-1 promotes neuronal cell death in ischemic stroke. Neurobiol Dis 2014; 62: 286-295.
[7] Salceda S and Caro J. Hypoxia-inducible factor 1 alpha (HIF-1 alpha) protein is rapidly degraded by the ubiquitin-proteasome system under normoxic conditions - Its stabilization by hypoxia depends on redox-induced changes. J Biol Chem 1997; 272: 22642-22647.
[8] Wang HC, Huang XN, Zhang JR, Shao N, Chen LO, Ma DX and Ji CY. The expression of VEGF and D114/Notch pathway molecules in ovarian cancer. Clin Chim Acta 2014; 436: 243-248.
[9] Zheng X, Linke S, Dias JM, Zheng X, Gradin K, Wallis TP, Hamilton BR, Gustafsson M, Ruas JL, Wilkins S, Bilton RL, Brismar K, Whitelaw ML, Pereira T, Gorman JJ, Ericson J, Peet DJ, Lendahl U and Poellinger L. Interaction with factor inhibiting HIF-1 defines an additional mode of cross-coupling between the Notch and hypoxia signaling pathways. Proc Natl Acad Sci U S A 2008; 105: 3368-3373.
[10] Gustafsson MV, Zheng XW, Pereira T, Gradin K, Jin SB, Lundkvist J, Ruas JL, Poellinger L, Lendahl U and Bondesson M. Hypoxia requires Notch signaling to maintain the undifferentiated cell state. Dev Cell 2005; 9: 617-628.
[11] Gao W, Sweeney C, Connolly M, Kennedy A, Ng CT, McCormick J, Veale DJ and Fearon U. Notch-1 mediates hypoxia-induced angiogenesis in rheumatoid arthritis. Arthritis Rheum 2012; 64: 2104-2113.
[12] Ma C, Wu GY, Wang ZL, Wang PH, Wu LM, Zhu GX and Zhao HQ. Effects of chronic sleep deprivation on the extracellular signal-regulated kinase pathway in the temporomandibular joint of rats. PLoS One 2014; 9.
[13] Sun C, Li JM, Wang B, Shangguan JJ, Figini M, Shang N, Pan L and Zhang ZL. Tumor angiogenesis and bone metastasis - Correlation in invasive breast carcinoma. J Immunol Methods 2018; 452: 46-52.
[14] Janusz MJ, Bendele AM, Brown KK, Taiwo YO, Hsieh L and Hietmeyer SA. Induction of osteoarthritis in the rat by surgical tear of the meniscus: inhibition of joint damage by a matrix metalloproteinase inhibitor. Osteoarthritis Cartilage 2002; 10: 785-791.
[15] Saito M, Sasho T, Yamaguchi S, Ikegawa N, Akagi R, Muramatsu Y, Mukoyama S, Ochiai N, Nakamura J, Nakagawa K, Nakajima A and Takahashi K. Angiogenic activity of subchondral bone during the progression of osteoarthritis in a rabbit anterior cruciate ligament transection model. Osteoarthritis Cartilage 2012; 20: 1574-1582.
[16] Mapp PI, Avery PS, McWilliams DF, Bowyer J, Day C, Moores S, Webster R and Walsh DA. Angiogenesis in two animal models of osteoarthritis. Osteoarthritis Cartilage 2008; 16: 61-69.
[17] Walsh DA, Bonnet CS, Turner EL, Wilson D, Situ M and McWilliams DF. Angiogenesis in the synovium and at the osteochondral junction in osteoarthritis. Osteoarthritis Cartilage 2007; 15: 743-751.
[18] Walsh DA, McWilliams DF, Turley MJ, Dixon MR, Franses RE, Mapp PI and Wilson D. Angiogenesis and nerve growth factor at the osteochondral junction in rheumatoid arthritis and osteoarthritis. Rheumatology (Oxford) 2010; 49: 1852-1861.
[19] Sahara M, Hansson EM, Wernet O, Lui KO, Spater D and Chien KR. Manipulation of a VEGF-Notch signaling circuit drives formation of functional vascular endothelial progenitors from human pluripotent stem cells. Cell Res 2014; 24: 820-841.
[20] Slade GD, Diatchenko L, Bhalang K, Sigurdsson A, Fillingim RB, Belfer I, Max MB, Goldman D and Maixner W. Influence of psychological factors on risk of temporomandibular disorders. J Dent Res 2007; 86: 1120-1125.
[21] LeResche L, Mancl LA, Drangsholt MT, Huang G and Von Korff M. Predictors of onset of facial pain and temporomandibular disorders in early adolescence. Pain 2007; 129: 269-278.
[22] Wu GY, Chen L, Zhu GX, Su YC, Chen YJ, Sun J and Wang YL. Psychological stress induces alterations in temporomandibular joint ultrastructure in a rat model of temporomandibular disorder. Oral Surg Oral Med Oral Pathol Oral Radiol Endod 2011; 112: e106-12.
[23] Fang W, Friis TE, Long X and Xiao Y. Expression of chondromodulin-1 in the temporomandibular joint condylar cartilage and disc. J Oral Pathol Med 2010; 39: 356-360.
[24] Li QF and Rabie AB. A new approach to control condylar growth by regulating angiogenesis. Arch Oral Biol 2007; 52: 1009-1017.
[25] Ehebauer M, Hayward P and Martinez-Arias A. Notch signaling pathway. Sci STKE 2006; 2006: cm7.
[26] Stenzel D, Franco CA, Estrach S, Mettouchi A, Sauvaget D, Rosewell I, Schertel A, Armer H,

Domogatskaya A, Rodin S, Tryggvason K, Collinson L, Sorokin L and Gerhardt H. Endothelial basement membrane limits tip cell formation by inducing Dll4/Notch signalling in vivo. Embo Reports 2011; 12: 1135-1143.

[27] Li ZQ, Wang J, Gong LL, Wen ZH, Xu CS and Huang XD. Correlation of delta-like ligand 4 (DLL4) with VEGF and HIF-1 alpha expression in human glioma. Asian Pac J Cancer Prev 2011; 12: 215-218.

[28] Shankar J, Thippegowda PB and Kanum SA. Inhibition of HIF-1 alpha activity by BP-1 ameliorates adjuvant induced arthritis in rats. Biochem Biophys Res Commun 2009; 387: 223-228.

[29] Yamaguchi A, Tojyo I, Yoshida H and Fujita S. Role of hypoxia and interleukin-1 beta in gene expressions of matrix metalloproteinases in temporomandibular joint disc cells. Arch Oral Biol 2005; 50: 81-87.

[30] Karlsson C, Brantsing C, Egell S and Lindahl A. Notch1, Jagged1, and HES5 are abundantly expressed in osteoarthritis. Cells Tissues Organs 2008; 188: 287-298.

[31] Mahjoub M, Sassi N, Driss M, Laadhar L, Allouche M, Hamdoun M, Ben Romdhane K, Sellami S and Makni S. Expression patterns of Notch receptors and their ligands in human osteoarthritic and healthy articular cartilage. Tissue Cell 2012; 44: 182-194.

[32] Nitzan DW. Intraarticular pressure in the functioning human temporomandibular-joint and its alteration by uniform elevation of the occlusal plane. J Oral Maxillofac Surg 1994; 52: 671-679.

[33] Cernanec J, Guilak F, Weinberg JB, Pisetsky DS and Fermor B. Influence of hypoxia and reoxygenation on cytokine-induced production of proinflammatory mediators in articular cartilage. Arthritis Rheum 2002; 46: 968-975.

[34] Chang J, Jackson SG, Wardale J and Jones SW. Hypoxia modulates the phenotype of osteoblasts isolated from knee osteoarthritis patients, leading to undermineralized bone nodule formation. Arthritis Rheumatol 2014; 66: 1789-99.

[35] Chen CW and Chen YQ. Experiment research on the influence of Yanghe decoction on the expression of HIF-1alpha mRNA in osteoarthritis. Zhongguo Gu Shang 2008; 21: 432-4.

[36] Hefler LA, Zeillinger R, Grimm C, Sood AK, Cheng WF, Gadducci A, Tempfer CB and Reinthaller A. Preoperative serum vascular endothelial growth factor as a prognostic parameter in ovarian cancer. Gynecol Oncol 2006; 103: 512-517.

[37] Mould AW, Tonks ID, Cahill MM, Pettit AR, Thomas R, Hayward NK and Kay GF. Vegfb gene knockout mice display reduced pathology and synovial angiogenesis in both antigen-induced and collagen-induced models of arthritis. Arthritis Rheum 2003; 48: 2660-266.

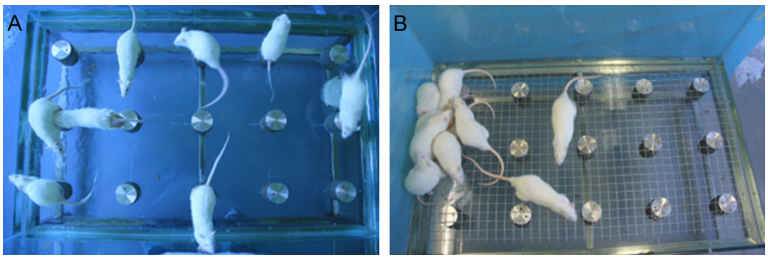

Figure S1. The experimental tank contained 15 small platforms for SD groups (A) or a grid for CN groups (B). (A) The rats on the small platforms could jump from one to another, but when they reached the paradoxical phase of sleep, their faces would touch the water as the muscle atonia. Thus, the rats in the small platforms suffered from sleep deprivation continuously, (B) the rats on the grid could lie down and sleep despite their tails might touch the water.

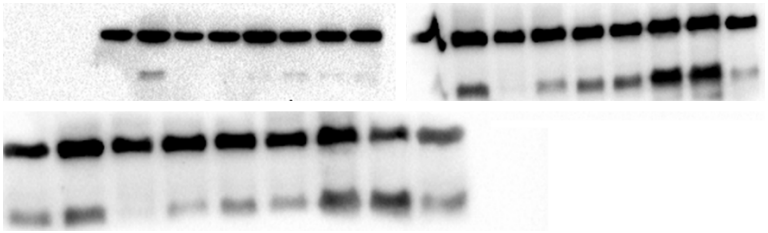

Figure S2. Representative original western images for β-actin including the whole membranes in rats experiment.

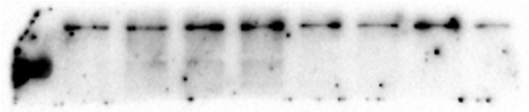

Figure S3. Representative original western images for Notch including the whole membranes in rats experiment.

Figure S4. Representative original western images for β-actin including the whole membranes in cell experiment.

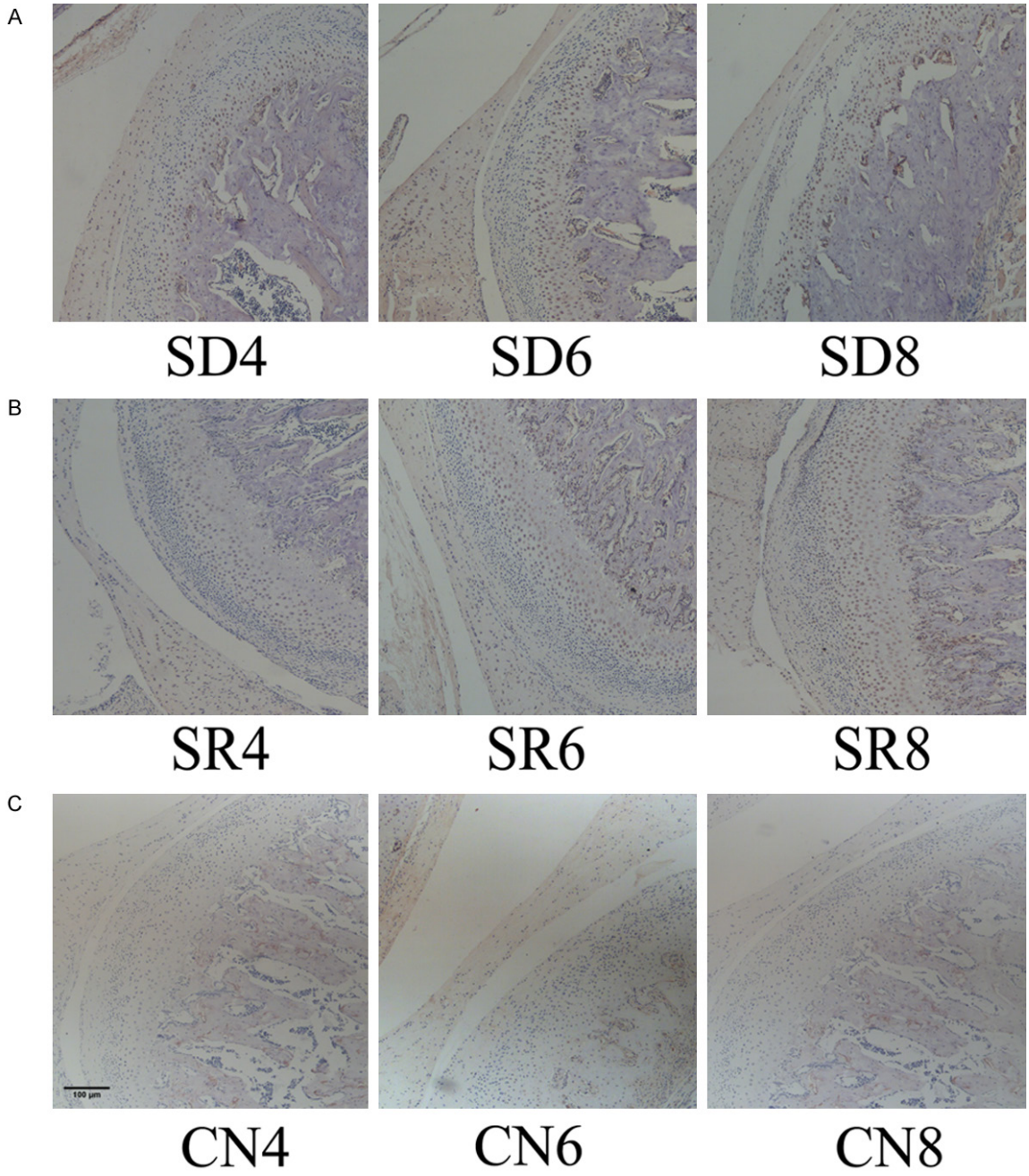

Figure S5. Representative images of immunohistochemistry staining for HIF-1α in the CN, SD SR groups respectively.

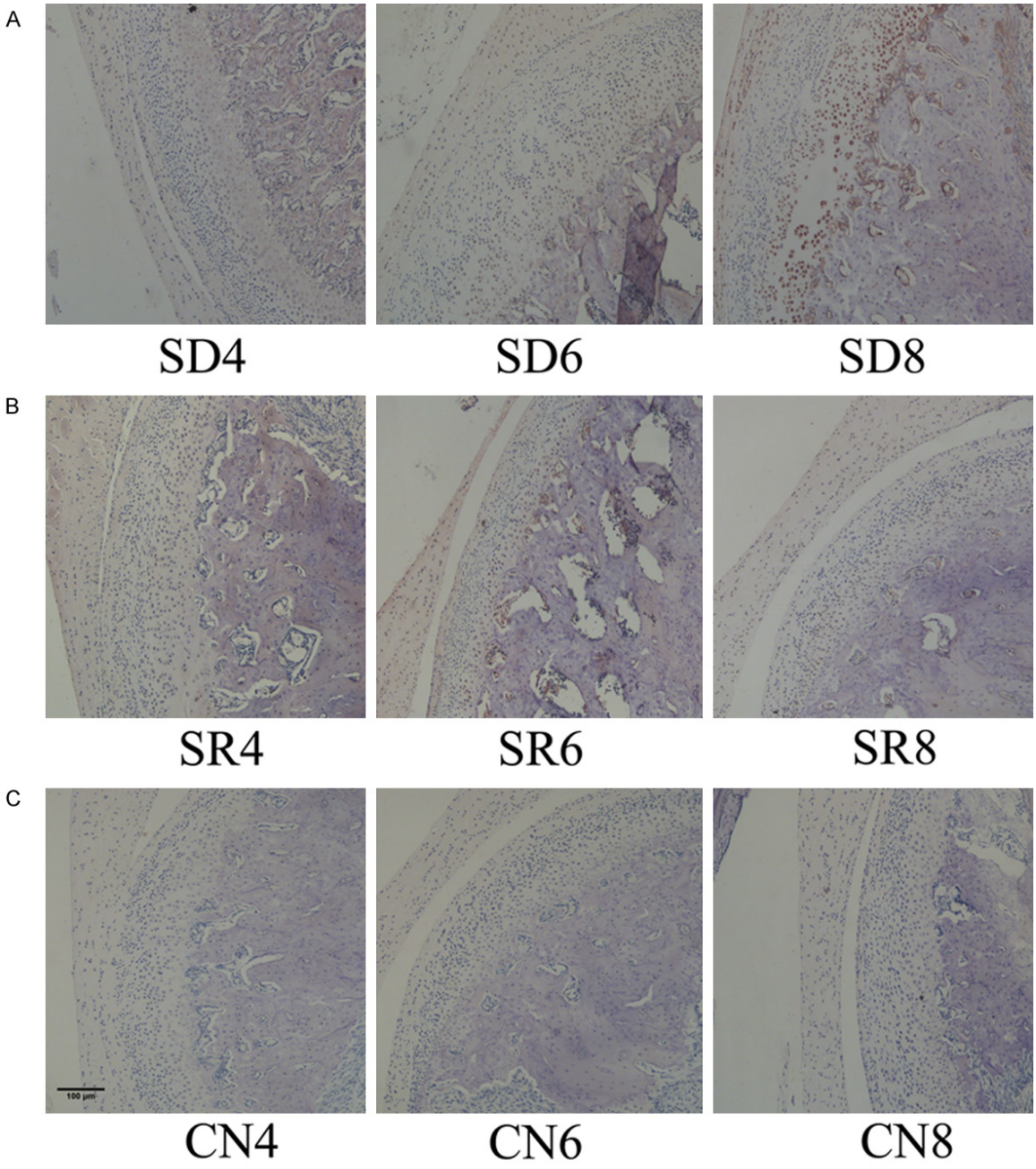

Figure S6. Representative images of immunohistochemistry staining for NICD in the CN, SD SR groups respectively.

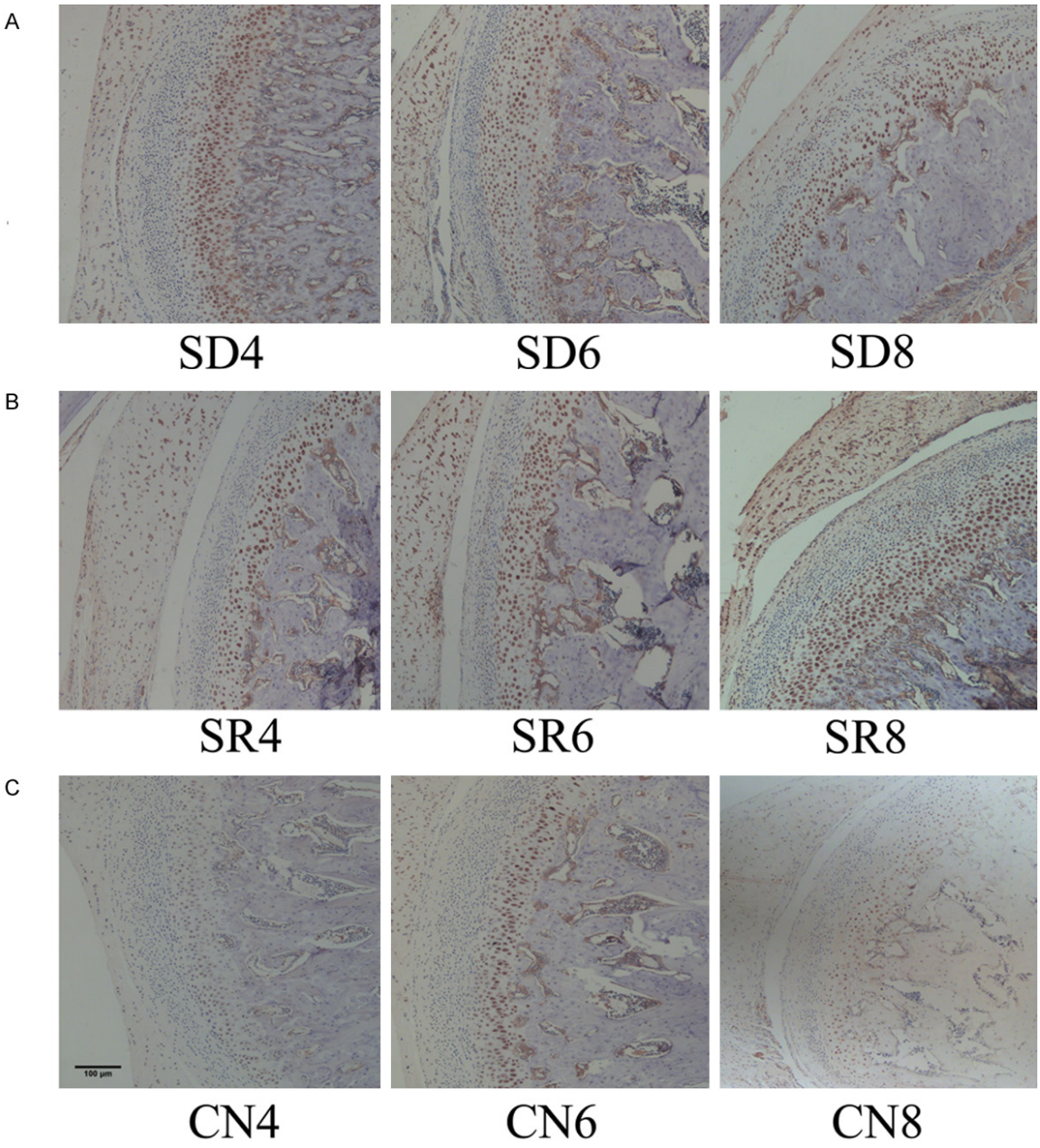

Figure S7. Representative images of immunohistochemistry staining for VEGF in the CN, SD SR groups respectively.